



Enhancement of base conductivity via the piezoelectric effect in AlGa_N/Ga_N HBTs

P.M. Asbeck*, E.T. Yu, S.S. Lau, W. Sun, X. Dang, C. Shi

University of California at San Diego, La Jolla, CA 92093-0407, USA

Received 23 May 1999; received in revised form 29 June 1999; accepted 18 August 1999

Abstract

Large polarization effects in nitride-based heterostructures provide opportunities for controllably introducing negative charge, equivalent to acceptor-doping, in AlGa_N/Ga_N HBT structures. This paper reviews evidence for polarization-based doping effects in nitride-based materials, and discusses potential applications of these effects for the improvement of p-contacts and p-type base conductivity. It is shown that in conventional HBTs grown with Ga-terminated faces in the emitter-up configuration, the polarization-induced charges detract from the acceptor doping of the base. In contrast, the polarization effects add to effective doping in the base in structures that are grown and processed as collector-up devices, or in devices that are grown emitter-up and utilize the transferred substrate approach. © 2000 Published by Elsevier Science Ltd. All rights reserved.

1. Introduction

The development of heterojunction bipolar transistors in Ga_N and related materials is an important research objective. Potential advantages of HBTs with respect to HFET structures in microwave power amplifier applications, for example, include high power density, higher transconductance, higher linearity, reduced sensitivity of device properties to the characteristics of surfaces or buffer layers, and the ability to conveniently tailor the bandstructure of the device along the direction of electron flow thereby facilitating the use of high bandgap alloys where fields are particularly high, the inclusion of ballistic launching ramps, or other strategies. Initial device demonstrations have been promising [1,2], but have highlighted the difficulty of producing adequate conductivity in the p-type base

layer of the transistors. This difficulty arises from the large ionization energy of typical acceptor impurities such as Mg; the tendency for compensation of acceptors to occur due to various species such as H; and the low mobility for holes in the nitrides, particularly in heavily-doped material. It has been recognized that the prominent spontaneous polarization and piezoelectric characteristics of the nitride semiconductors offer a potential approach to mitigate these problems, by appropriately controlling the device strain and polarization. This paper reviews experimental evidence relevant to such polarization-based doping, and presents several strategies for the improvement of both base contacts and base hole conductivity.

2. Polarization effects in nitrides

Recent theoretical and experimental work has highlighted the fact that the nitride-based semiconductors exhibit very strong polarization, comprising both spon-

* Corresponding author. Fax: +1-619-534-0556.

E-mail address: asbeck@ece.ucsd.edu (P.M. Asbeck).

Table 1
Selected physical constants for GaN, AlN, and InN

	GaN	AlN	InN	Reference
a (Å)	3.189	3.112	3.548	8
c (Å)	5.185	4.982	5.760	8
e_{31} (C/m ²)	-0.32			9
e_{31} (C/m ²)	-0.22			10
e_{31} (C/m ²)	-0.36			11, 12
e_{31} (C/m ²)		-0.58		13
e_{31} (C/m ²)	-0.49	-0.60	-0.57	7
e_{33} (C/m ²)	0.65			9
e_{33} (C/m ²)	0.44			10
e_{33} (C/m ²)	1			11, 12
e_{33} (C/m ²)		1.55		13
e_{33} (C/m ²)	0.73	1.46	0.97	7
$P_{sp,z}$ (C/m ²)	-0.029	-0.081	-0.032	7

taneous polarization, and strain-induced (piezoelectric) polarization components [3–7]. The strain effects are important in nitride heterostructures because of the lattice-mismatch between the components materials such as GaN, AlN and InN and their alloys. For epitaxial growth along the c axis of wurtzite crystals, the overall polarization P_{tot} in a layer is directed along the c -axis and has a value given by

$$P_{tot} = (e_{31} - c_{13}/c_{33} \cdot e_{33}) \cdot (\epsilon_{xx} + \epsilon_{yy}) + P_{spont} \quad (1)$$

where e is the piezoelectric stress tensor (expressed in contracted index notation), c is the elastic stiffness tensor, ϵ is the strain and P_{spont} is the spontaneous polarization (which is also directed along the c -axis).

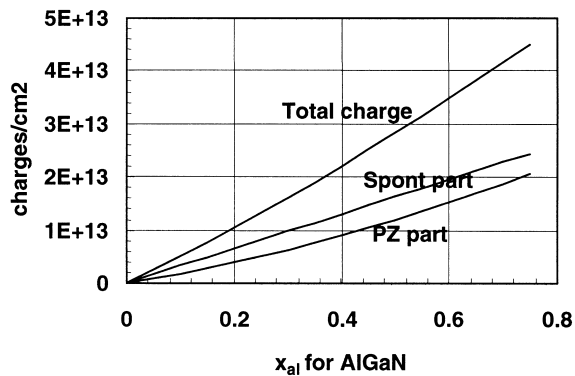


Fig. 1. Calculated values of interface sheet charge (expressed in units of electron charge) for thin AlGaIn layers deposited on GaN buffer layers, as a function of Al mol fraction. The AlGaIn layer is assumed to accommodate to the lattice-constant of GaN. Charges densities arising from spontaneous polarization and from piezoelectric effects individually are also shown.

The precise values of the material constants to be used in Eq. (1) are not known with certainty, but estimates have been provided by a number of authors. Table 1 lists, for example, a variety of values from the literature [8–13]. The piezoelectric coefficients are more than five times higher than in GaAs. The sign of e_{33} is opposite to that found in the zincblende III–V compounds (after translating the values determined for the cubic crystals to the hexagonal structure) and in agreement with that found in wurtzite II–VI compounds. As a result of spatially-varying polarization in crystals, a bound charge density ρ_{pol} is produced, given by

$$\rho_{pol} = -\nabla \cdot P. \quad (2)$$

This polarization-induced charge acts as a source of electrostatic fields along with free charges (electrons and holes) and charged impurities. As a consequence, at the interface of two layers with polarizations P_1 and P_2 , a polarization induced sheet charge density $Q_s = P_1 - P_2$ is produced. This sheet charge can have appreciable magnitude. Fig. 1 plots, for example, the sheet charge density Q_s (expressed as $N_s = Q_s/q$) obtained at the interface between AlGaIn and GaN, assuming that the AlGaIn accommodates to the lattice constant of GaN. In the computation of the values shown in this figure, the piezoelectric coefficients were estimated to be an average of the various determinations of Table 1. The sheet charge density reaches values of the order of 10^{13} cm⁻². The variation of N_s with aluminum concentration is not linear because of the estimated change in piezoelectric coefficients with alloy composition.

It should be noted that the charge associated with the interface does not (to lowest order) depend on the state of stress of the GaN layer itself, only on the difference in strain between the GaN and the overlying AlGaIn layer. “Common-mode” strains, i.e. those that affect both the buffer-layer and overlying AlGaIn layer, cancel out in the determination of interface charge.

3. Piezoelectronic doping

The bound charge associated with the divergence of the polarization may be viewed as a source of charge analogous to ionized impurities. This charge can be intentionally incorporated into nitride-based heterostructures for various device design purposes, such as inducing the presence of electron or hole densities. The positive charge resulting from the polarization changes exhibits in many respects donor-like behavior, while the negative charge is, correspondingly, acceptor-like. The incorporation of the piezoelectronic charge represents another design variable that may be used for

the optimization of structures. Such “piezoelectronic doping” obeys several rules, including the following:

1. The overall system is constrained to be neutral. Thus piezoelectronically-produced donors and acceptors occur in equal numbers. The doping effects of piezoelectronic engineering thus can be better described as the controlled incorporation of dipoles rather than of monopoles.
2. The sign of the charge obtained is dependent on the orientation of the crystal. Epitaxial layers grown with Ga-terminated faces (0001 orientation) contain polarization dipoles opposite in orientation to those grown with N-terminated faces (000 $\bar{1}$ orientation).
3. The piezoelectronic “dopants” are always fully ionized. There is no possibility of binding of electrons or holes to the polarization-induced charge, since it is dispersed over surfaces or volumes. This feature is of significant benefit in the nitrides, for which impurity acceptors have large binding energies, and, consequently, relatively low ionization ratios at room temperature.
4. The piezoelectronic “dopants” do not produce ionized impurity scattering. Since there are no localized centers for electrons to scatter from, with ideal planar interfaces and uniform materials the presence of piezoelectronic doping should not decrease mobility. This feature is identical to that of modulation doping. In real crystals in which interfaces are rough and alloy compositions fluctuate, however, there will be distributions of piezoelectrically-induced charge that can cause scattering and mobility reduction.

3.1. Limitations due to stress relaxation

The maximum value of piezoelectronic doping that can be incorporated into a device is limited by the maximum strain that can be present within the lattice-mismatched layers. In the growth of heteromorphic layers in many III–V compounds such as GaAs and InP, it is well established that if a critical layer thickness is exceeded in lattice-mismatched growth, misfit dislocations will form and result in partial to complete strain relaxation. The experimental results in the nitride-based semiconductors are less clear. The hexagonal wurtzite crystals do not permit glide of dislocations as readily as the zincblende structures. As a result, the mechanical equilibrium situation may not be reached in most samples. Bykhovski et al. [14] have reported a computation of critical thickness for AlGa \bar{N} layers on Ga \bar{N} buffers, indicating approx. 200 Å critical thickness for 15% aluminum. Experimental data inferred from C – V measurements of piezoelectronic charge suggest that much thicker layers can be pro-

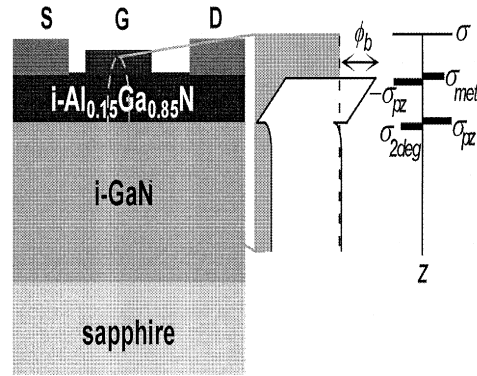


Fig. 2. Schematic structure of AlGa \bar{N} /Ga \bar{N} HFET, together with corresponding band diagram and charge densities.

duced at that aluminum concentration while still incorporating substantial strain [14]. It is possible that in many nitride-based samples the strain levels can be built up until the onset of cracking.

Large densities of c -axis oriented threading dislocations are present in most nitride samples. It has been shown that there are polarization components associated with the strain fields of these dislocations. However, the divergence of the polarization vanishes for c -axis oriented dislocations almost everywhere. Charges arise from the dislocation strain fields only at surfaces and interfaces, in the case of dislocations with an edge component [15].

3.2. Limitations due to compensation

It can be expected that the piezoelectronic “doping” will be partially compensated by native defects and impurities during crystal growth and subsequent processing. While the piezoelectronic charge is not localized, and will not create bonding interactions and undergo complex formation (such as Mg incorporation in Mg–H complexes), the effect of the piezoelectronic charge on the Fermi level will contribute to decreasing the energy of formation of defects, thereby increasing their density. Walukiewicz [16] has simulated the increase of native donors in AlGa \bar{N} /Ga \bar{N} HFETs as a result of the presence of “piezoelectronic acceptors” at the surface of growing heterostructures. It is also possible that hydrogen incorporation as H⁺ entities will be increased at the surface as piezoelectronic acceptors are incorporated into the material, since they are energetically strongly favorable as the Fermi level in the semiconductor approaches the valence band. The degree of compensation obtained under different growth conditions is not yet known. Under worst case scenarios, the compensation will negate the formation of p-type conductivity. An attractive scenario, already proposed by Van Vechten [17] to explain the p-type

conductivity resulting from Mg doping, is that H^+ may compensate the acceptors during growth to an extent that discourages the incorporation of more stable donor-like centers. Subsequently, the hydrogen may be expelled during relatively low temperature anneals to activate the acceptors.

3.3. Piezoelectronic doping effects in HFETs

It has been recently demonstrated that piezoelectronic doping effects have a major role in the establishment of carrier densities in AlGaIn/GaN HFET structures [5,6]. Fig. 2 shows the structure of a representative HFET. The spontaneous polarization and piezoelectric polarization within this structure are oriented primarily along the growth direction and undergo an abrupt change at the AlGaIn/GaN interface, producing a donor-like sheet charge at that interface. A corresponding negative sheet charge is produced at the surface of the wafer, as indicated in Fig. 2. The negative surface charge is compensated by the charge on a Schottky metal gate, while the charge at the AlGaIn/GaN interface is compensated by electrons which form a 2-dimensional electron gas (apart from a net charge component that must remain to terminate the electric field between gate and 2 DEG). For a free surface rather than a Schottky metal, a similar situation will arise, assuming that there are compensating charges at the surface as a result of surface states, impurities or charged native defects near the surface, or external charged entities. Experimental evidence suggests that the surface potential for a free surface is lower than produced with metal Schottky barriers, and the electric field between channel and surface is small. The 2 DEG density in HFET structures produced by polarization charges is then expected to be equal to the

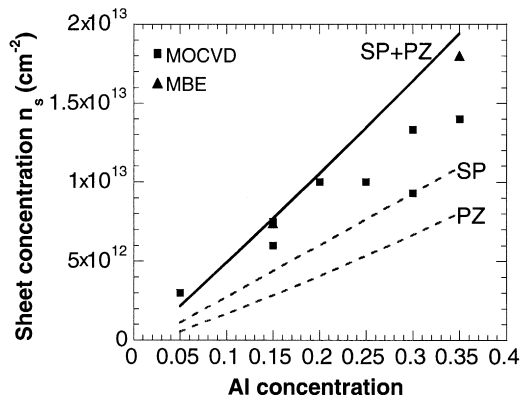


Fig. 3. Comparison between experimental values of sheet carrier concentration in HFET structures, obtained from Hall measurements, and predictions of polarization-based model. The HFET structures did not have intentional doping.

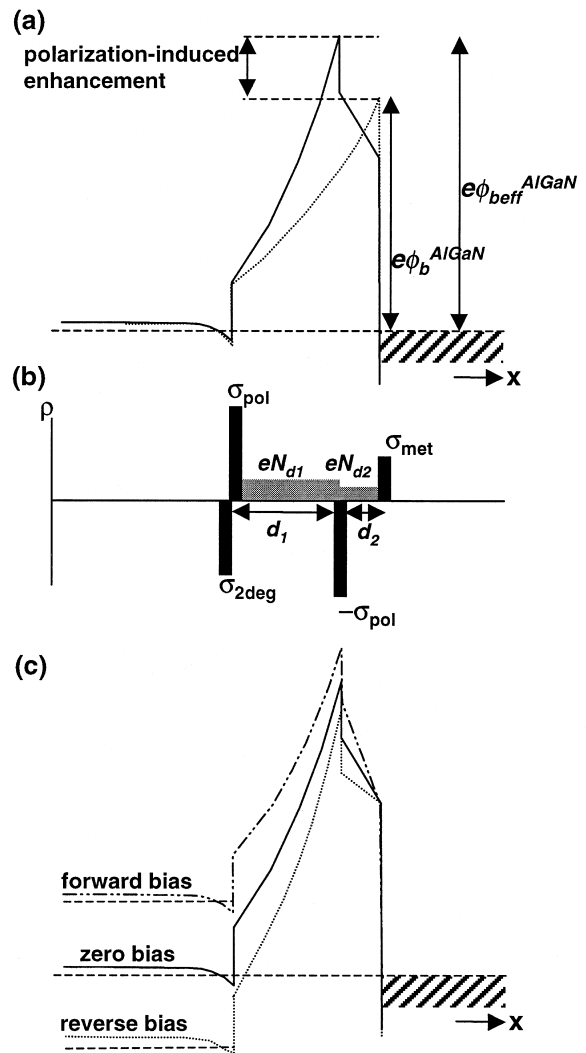


Fig. 4. (a) Band diagram for enhanced Schottky barrier structure via piezoelectronic doping. (b) Schematic charge densities. (c) Behavior of the band diagram as the Schottky barrier voltage is changed.

piezoelectronic charge density of Fig. 1. In Fig. 3 are plotted experimental values of sheet electron density obtained by Hall measurements for nominally undoped HFET layer structures as a function of aluminum mol fraction, together with the predictions of the preceding analysis. Layers grown by both MOCVD and by MBE are represented in these data. There is reasonable agreement between the analysis and experiment, although at high Al mol fractions the discrepancies are greater. The agreement between analysis and experiment is no doubt influenced by possible strain relaxation, by incorporation of unintentional dopants (particularly donors), and imprecise knowledge of aluminum mol fraction in the samples.

3.4. Enhancement of Schottky barrier height in HFET structures

The possibility of control over electrostatic charge distribution through piezoelectric engineering has led to some novel structures. One example is provided by a structure intended to increase the effective barrier height of the Schottky gate within an HFET structure [18]. An increase in barrier height can in principle be obtained by the incorporation of acceptor-like charge near the Schottky gate. In the conventional camel diode, this charge is produced by incorporation of acceptor impurities. Recently, structures have been fabricated where the enhancements were produced by the use of piezoelectric acceptors. The overall layer structure consists of a layer of GaN on top of an AlGaN layer, which is on top of a GaN buffer layer. Fig. 4 depicts the structure, charges, and expected band diagram. The barrier height is increased by the amount of potential drop in the surface GaN layer, which in turn is dependent on the piezoelectric acceptor charges at the top GaN/AlGaN interface. Photoresponse measurements of barrier height have been made for samples prepared in this manner [18]. The observed results indicated that the barrier height was enhanced by up to 0.37 eV, for samples employing AlGaN layers of 25% aluminum mol fraction, at zero bias. As is expected for camel diodes, the barrier height is somewhat dependent on the voltage applied to the Schottky diode, and increases for forward bias, as shown in Fig. 4(c). The measured barriers are in approximate accord with the values predicted with a simple analysis (which assumes that the material has residual unintentional donors at a level of $1 \times 10^{18} \text{ cm}^{-3}$). Samples prepared with 30% aluminum mol fraction exhibited a barrier enhancement of 0.27 eV, which agrees less well with the predictions, suggesting that lattice-relaxation may have had a role.

4. Piezoelectric enhancement of base contacts

The high specific contact resistance of ohmic contacts to p-type GaN and nitride heterostructure layers has been a persistent problem for the development of HBTs as well as LEDs and lasers. As reported elsewhere in this issue, values of the order of 10^{-4} ohm cm^2 are typical of the best reported in HBT structures, and frequently much higher values are obtained. There is significant promise with the emerging Ti/Ta contacts, although work remains to demonstrate stability over time. It would be very valuable to enhance p-ohmic contact performance via polarization effects. Here we show a design that in principle should significantly enhance the contact behavior. The proposed mechanism for enhancement is to create piezoelectric nega-

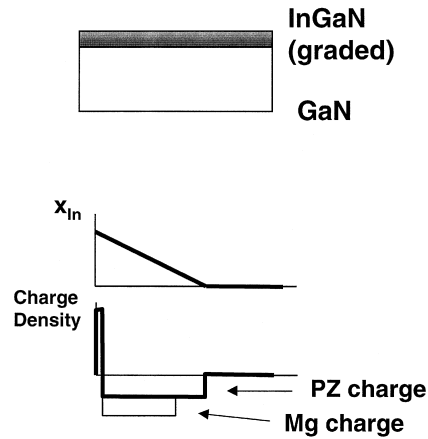


Fig. 5. (a) Layer structure for p-type ohmic contact enhanced via piezoelectric doping. (b) Corresponding indium alloy composition vs depth, and charge density.

tive (acceptor-like) charge in the vicinity of the surface, where it can contribute to thinning of the depletion region, and enhance the tunneling probability of holes. The piezoelectric charge can be established with the use of a layer of InGaN deposited on a GaN substrate. A graded composition is used in order to distribute the charge over a finite width. The proposed structure is illustrated in Fig. 5. The surface layer is also doped with Mg. A conventional ohmic contact may be represented in approximate fashion as an ideal Schottky barrier, in which the depletion region is thin enough to permit tunneling of electrons whose initial energy is near the fermi level or somewhat close to it (corresponding to thermionic field emission current). Fig. 6 shows the predicted valence band diagrams for a structure with and without piezoelectric charge. The In composition of the InGaN contact layer is graded from 0 to 15% at the surface of a layer 60 Å thick. A Schottky barrier height of 2.2 eV has been assumed. The figure shows that significant thinning of the depletion layer occurs, which should lead to enhanced

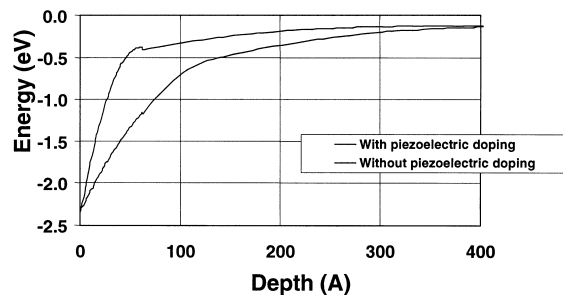


Fig. 6. Calculated valence band profile for piezoelectronically enhanced p-contact, and corresponding calculation if piezoelectric effects are omitted.

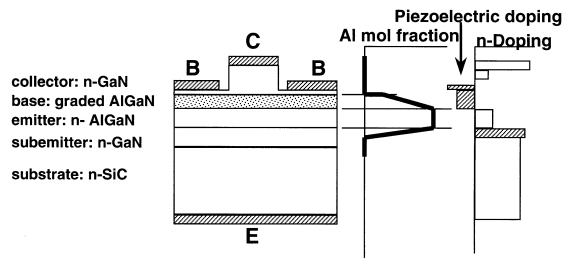


Fig. 7. Schematic structure of emitter-up HBT, along with aluminum mol fraction as a function of depth, and schematic charge densities.

current flow at a given bias. In the simulation, Mg has been assumed not to be complexed with hydrogen, and to have an acceptor depth of 0.18 eV. Ionization of the Mg is enhanced in the vicinity of the contact as a result of band-bending. Experiments are underway to investigate this effect in real structures.

5. Piezoelectronic enhancement of HBT base layer conductivity

The use of piezoelectronic doping to increase the hole concentration within the base of AlGaIn/GaN HBTs is an attractive possibility, particularly since it should be achievable without incurring a penalty in hole mobility. The polarization change between an AlGaIn emitter and a GaN base provides such a possibility. Corresponding designs are discussed in the following, for devices which are grown in an emitter-up configuration, and in a collector-up configuration. The transferred substrate HBT, which may be grown in a collector-up configuration and processed in an emitter-up configuration, is also discussed.

5.1. Emitter-up HBTs

At the interface between an emitter layer of AlGaIn and a base of GaN, a piezoelectric sheet charge may be formed, which can lead to the formation of a two-dimensional hole gas. It is also possible to grade the aluminum composition over a finite thickness, thus providing an equivalent acceptor doping over a finite region. These concepts are shown in the schematic layer design shown in Fig. 7.

The magnitude of the maximum base sheet charge that can be generated on this basis is in the range $1\text{--}3 \times 10^{13} \text{ cm}^{-2}$. For example, for an AlGaIn emitter layer with 25% Al and a base of GaN, the aggregate charge is estimated to be $1.4 \times 10^{13} \text{ cm}^{-2}$ (which may be localized in a sheet, or spread over an appreciable distance depending on the grading of the Aluminum content). If distributed over a base of width 500 Å, this would

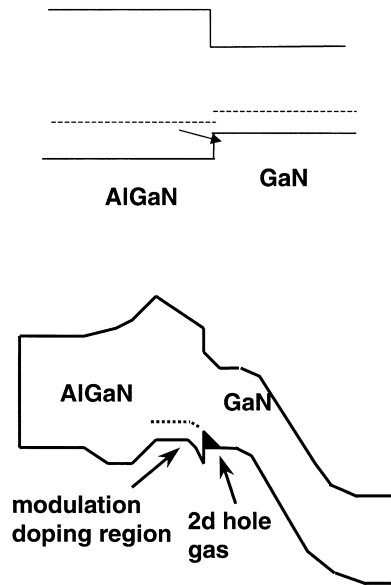


Fig. 8. Schematic band diagram near AlGaIn–GaN interface, illustrating modulation doping effect to decrease ionization energy of Mg acceptors. A schematic band diagram of an emitter-up HBT with enhanced base conductivity is also shown.

correspond to a value p-type dopant concentration of $2.8 \times 10^{18} \text{ cm}^{-3}$. The polarization-induced charge can be increased to a value of about $4 \times 10^{13} \text{ cm}^{-2}$ with the addition of indium to the base (assuming an In content of the order of 10%), which would also allow higher aluminum concentration to be reached for a given degree of strain. The corresponding doping concentration over a 500 Å base is $8 \times 10^{18} \text{ cm}^{-3}$. However, the negative charge obtained in practice may be lower as a result of strain-relaxation or compensation, as noted above.

The magnitude of the base charge desired in a bipolar transistor is of this same magnitude or greater, and is necessary to impart sufficient conductivity to the base, as well as to support the electric fields from the collector. If the maximum base sheet resistance is taken to be 20,000 ohm/square (acceptable only if the emitter width is small), then the required base sheet doping is of order $1.6 \times 10^{13} \text{ cm}^{-2}$, assuming a hole mobility of $20 \text{ cm}^2/\text{V s}$. Mobility of holes in the base could be greater with piezoelectronic doping than observed with Mg doping, as noted above. In order to terminate electric fields in the BC depletion region, values of sheet charge up to $1.7 \times 10^{13} \text{ cm}^{-2}$ are needed (assuming the transistor is to be operated without base punchthrough up to the onset of avalanche breakdown with a field of 2.5 MV/cm). Higher values of base sheet doping would result in further improvement of key device characteristics.

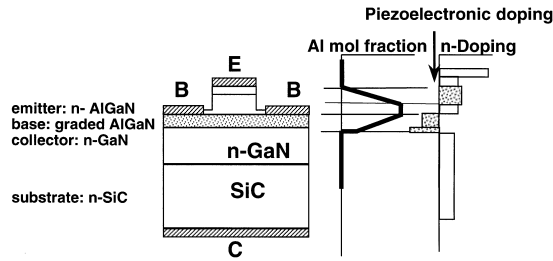


Fig. 9. Simulated distribution of hole density in the base region of an AlGaIn/GaN emitter-up HBT, with piezoelectronically-enhanced charge as well as Mg-doping. The concentration of ionized Mg impurities is also shown, illustrating the enhancement near the base-collector junction and at the AlGaIn/GaN interface.

These considerations indicate that it would be desirable and perhaps necessary to supplement the piezoelectric acceptor doping with acceptor impurity doping, such as with Mg. In the vicinity of the BC junction, for example, the variation of electrostatic potential should cause the Mg to be fully ionized within the depletion region, essentially eliminating the problem of punchthrough. The depth of the Mg acceptor could nonetheless create problems due to the finite emission rate of holes from the acceptor level, so that the time response of the impurity doping in the base may be insufficient for high frequency signals.

When incorporating the Mg doping in the suggested structure, it is convenient to take advantage of the modulation doping capabilities of the heterojunction. For example, if the acceptor depth within AlGaIn is the same as in GaN, or at least does not increase by the full amount of the valence band difference ΔE_v between these two materials, then it will be energetically advantageous for Mg acceptors in the AlGaIn layer to ionize by providing holes to the valence band of GaN in the neighboring layer, as shown schematically in Fig. 8. With the use of a single interface between AlGaIn and GaN (rather than a superlattice) there are no barriers to electron flow introduced. The band diagram for the proposed structure is shown in Fig. 8. Fig. 9 shows the simulated hole density as a function of depth, along with the ionization fraction expected for the Mg. The figure illustrates that a sizeable hole density of about $1.5 \times 10^{13} \text{ cm}^{-2}$ is attained, and that the ionization of the Mg is enhanced in the vicinity of the AlGaIn/GaN interface and at the BC junction. The calculated dependence of the base sheet charge on base-collector voltage shows that very little change ($<10\%$) in the base sheet concentration occurs up to collector voltages approaching avalanche breakdown. This variation is sufficiently low to avoid excess output conductance.

While the proposed design of the HBT base appears

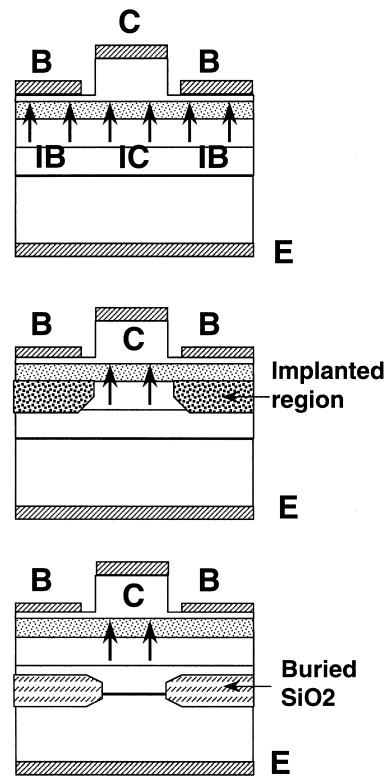


Fig. 10. Structure of collector-up HBT, along with aluminum mol fraction vs depth, and schematic charge densities.

to be useful for applications, it should be emphasized that in order for the piezoelectronically produced charges to have the proper sign in the base, to act as acceptors rather than donors, it is necessary for the epitaxial layers to be grown with a N-terminated face, that is a 000 $\bar{1}$ growth direction. This is opposite to the crystal polarity typically achieved in nitride growths. By contrast, with the usual crystal orientation, the piezoelectrically defined charges are donor-like, and subtract from the Mg doping of the base. This situation is believed to occur in the GaN-based HBTs reported to date, and is potentially one of the significant barriers to the operation of those devices.

In order to produce piezoelectric acceptors at the emitter base junction, while employing the conventional Ga-terminated 0001 growth, it is necessary to grow the structure with the emitter below the surface, next to the buffer, followed by the base, and finally the collector.

5.2. Transferred-substrate HBTs

Using the transferred substrate technique, it is possible to grow an epitaxial layer structure collector-up, and subsequently process it emitter-up, after transfer-

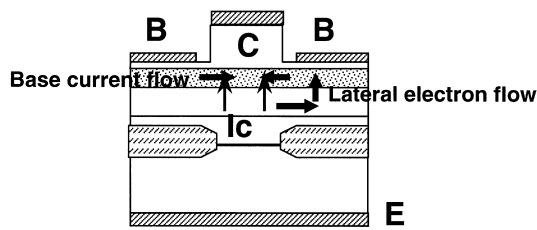


Fig. 11. Schematic current flow in collector-up HBT, illustrating loss of current gain due to extrinsic emitter regions. Also shown are structures to mitigate this effect. In (b) an implant of p material or compensating deep levels is shown. In (c), buried SiO₂ layers obtained from the LEO growth process are shown.

ring the wafer to an auxiliary handle substrate, and removing the original substrate used during growth. This technique has been used by Rodwell et al. [19] to achieve extremely high frequency performance in InP/InGaAs/InP. The advantages of this approach are detailed by Rodwell elsewhere in this issue. It is fortunate that the piezoelectronic doping features are also favorable in this geometry.

5.3. Collector-up HBTs

Another option for the fabrication of high performance HBTs is to process the structure with the collector at the wafer surface. Kroemer [20] pointed out that this geometry has the desirable feature of dramatically reduced base-collector capacitance (which is the most critical parasitic limiting high frequency performance). A schematic structure for a collector-up AlGaN/GaN HBT with piezoelectronically-enhanced base conductivity is shown in Fig. 10; the structure is a mirror-image of the emitter-up design. A well-known problem with the collector-up design, however, is the fact that regions of the emitter not covered by the device collector (“extrinsic emitter” regions), may inject minority carriers into the base, which will not be collected, but rather will contribute to base current. It is critical to suppress this extrinsic base current contribution in order to have adequate current gain. The problem is particularly severe for devices with narrow collectors, since the collector current scales as the collector area, while the extrinsic emitter base current scales as the collector periphery. There are a number of strategies that have been demonstrated in HBTs in other material systems that can be used to suppress the extrinsic current. One possibility, illustrated in Fig. 11(b), is based on the use of damage implants (or p-implants) to produce current blocking barriers in the emitter layers that lie underneath the base contacts. It is challenging, however, to produce such layers without adversely affecting the conductivity of the base layer

and the ohmic contact quality. Another strategy, illustrated in Fig. 11(c), is based on the use of buried layers of dielectric (such as SiO₂) that can eliminate the current in the side regions of the device. Such layers could potentially be introduced with the use of the Lateral Epitaxial Overgrowth technique, which has been employed to successfully eliminate threading dislocations in the overgrown regions. Our simulations indicate that in the design of transistor structures that make use of this technique, it is critical to avoid excess electron current in the emitter on top of the SiO₂ barrier, that could negate the “funneling effect” of the SiO₂ barrier. This requires that the AlGaN emitter layer on top of the SiO₂ be thin and have relatively low donor doping, or to be converted to p-type by implantation.

6. Summary

Large polarization effects in nitride semiconductors permit significant effective doping levels to be controllably introduced into heterostructures. It is expected that substantial improvements in base contacts, as well as significant enhancement in base hole concentration (up to $4 \times 10^{13} \text{ cm}^{-2}$) may be obtained with this technique. Addition of Mg or alternative acceptor impurity is also worthwhile. To obtain the benefit of this technique, the crystal polarity must be suitably chosen for the HBT geometry used. In devices reported to date, and emitter-up approach (together with a probable Ga-terminated growth) leads to a decrease, rather than enhancement of the base doping. A transferred substrate device or collector-up transistor has the structure desired to benefit from the polarization effects with Ga-terminated growth.

Acknowledgements

Financial support for this work has been provided by ONR (Dr J. Zolper), and by BMDO (Dr K. Wu). The authors gratefully acknowledge helpful discussions with U. Mishra, R. Davis, J. Speck, and M. Rodwell.

References

- [1] McCarthy L, Kozodoy P, Denbaars S, Rodwell M, Mishra U. First demonstration of an AlGaN/GaN heterojunction bipolar transistor. In: Int. Symp. Comp. Semiconductors, 1998.
- [2] Ren F, Abernathy C, Van Hove J, Chow P, Hickman R, Klaasen J, Kopf R, Cho H, Jung K, La Roche J, Wilson R, Han J, Shul R, Baca A, Pearton S. 300C GaN/

- AlGaIn heterojunction bipolar transistor. *Int J Nitride Sem Res* 1998;3:41.
- [3] Bykhovski A, Gelmont B, Shur M. The influence of the strain-induced electric field on the charge redistribution in GaN-AlN-GaN structure. *J Appl Phys* 1993;74:6734.
- [4] Martin G, Botchkarev A, Rockett A, Morkoc H. Valence-band discontinuities of wurtzite GaN, AlN and InN heterojunctions measured by X-ray photoemission spectroscopy. *Appl Phys Lett* 1996;68:2541.
- [5] Asbeck PM, Yu ET, Lau SS, Sullivan GJ, Van Hove Redwing J. Piezoelectric charge densities in AlGaIn/GaN HFETs. *Electronics Letters* 1997;33(4):1230–1.
- [6] Yu ET, Sullivan GJ, Asbeck PM, Wang CD, Qiao D, Lau SS. Measurement of piezoelectrically induced charge in GaN/AlGaIn heterostructure field-effect transistors. *Appl Phys Lett* 1997;71:2794.
- [7] Bernardini F, Fiorentini V, Vanderbilt D. Spontaneous polarization and piezoelectric constants of III-V nitrides. *Phys Rev B* 1997;56:R10024.
- [8] Strite S, Lin ME, Morkoc H. Progress and prospects for GaN and the III-V nitride semiconductors. *Thin Solid Films* 1993;231:197.
- [9] Littlejohn MA, Hauser JR, Glisson TH. Monte-Carlo calculation of the velocity-field relationship for GaN. *Appl Phys Lett* 1975;26:625.
- [10] Bykhovski AD, Kaminski VV, Shur MS, Chen QC, Khan MA. *Appl Phys Lett* 1996;68:818.
- [11] O'Clock Jr GD, Duffy MT. Acoustic surface wave properties of epitaxially grown AlN and GaN on sapphire. *Appl Phys Lett* 1973;23:55.
- [12] Bykhovski AD, Gelmont BL, Shur MS. *J Appl Phys* 1997;81:6332.
- [13] Gualtieri J, Kosinski JA, Ballato A. Piezoelectric materials for acoustic wave applications. *IEEE Trans Ultrason Ferroelec Freq Contr* 1994;41:53.
- [14] Bykhovski A, Gaska R, Shur MS. Piezoelectric doping and elastic strain relaxation in AlGaIn-GaN heterostructure field effect transistors. *Appl Phys Letts* 1998;73:3577–9.
- [15] Shi C, Asbeck PM, Yu ET. Piezoelectric polarization associated with dislocations in wurtzite GaN. *Appl Phys Lett* 1999;74:573.
- [16] Hsu L, Walukiewicz W. Effects of piezoelectric field on defect formation, charge transfer, and electron transport at GaN/Al_xGa_{1-x}N interfaces. *Appl Phys Letts* 1998;73:339–41.
- [17] Van Vechten JA, Zook JD, Horning RD, Goldenberg B. Defeating compensation in wide gap semiconductors by growing in H that is removed by low temperature deionizing radiation. *Japanese Journal of Applied Physics, Part 1* 1992;31:3662.
- [18] Yu ET, Dang XZ, Yu LS, Qiao D, Asbeck PM, Lau SS. Schottky barrier engineering in III-V nitrides via the piezoelectric effect. *Appl Phys Lett* 1998;73(13):1880.
- [19] Lee Q, Agarwal B, Mensa D, Pullela R, Guthrie J, Samoska L, Rodwell MJW. A >400 GHz f_{max} transferred-substrate heterojunction bipolar transistor IC technology. *IEEE Electr Dev Letts* 1998;19:77.
- [20] Kroemer H. Heterostructure bipolar transistors and integrated circuits. *Proc IEEE* 1982;70:13.